Journal of Geochemical Exploration 188 (2018) 111–122

Contents lists available at ScienceDirect

Journal of Geochemical Exploration

journal homepage: www.elsevier.com/locate/gexplo

Redox behaviour of arsenic in the surface sediments of the Marque River (Northern France)

Josselin Gorny[a], Gabriel Billon[a,*], Catherine Noiriel[b], David Dumoulin[a], Ludovic Lesven[a], Benoît Madé[c]

[a] LASIR; UMR CNRS 8516, University of Lille, Villeneuve d'Ascq, France
[b] Géosciences Environnement Toulouse, Observatoire Midi-Pyrénées, Université Paul Sabatier, CNRS, IRD, Toulouse, France
[c] French National Radioactive Waste Management Agency (Andra), Research and Development Division (DRD), Châtenay-Malabry, France

ARTICLE INFO

Keywords:
Arsenic
Early diagenesis
River sediment
Redox gradient
Redox speciation

ABSTRACT

The behaviour of arsenic(As) in anoxic sediments was studied in the Marque River (Northern France), where concentrations of As are close to the geochemical background level. The distribution of Fe, Mn, S and As species in the solid phase as well as in the pore waters was investigated during four sampling campaigns (February, April, July and October 2014) in order to better understand the parameters involved in the behaviour of arsenic during early diagenetic processes. In the solid phase, As was found to be mainly present in the exchangeable fraction, and the most probable As carrier phases appeared to be amorphous iron, manganese (hydr)-oxides, calcite, and siderite. In pore waters, only the inorganic forms of arsenic [As(III), As(V), and thio-arsenical species] were detected. As(III) was the dominant species, but thio-arsenic species were also evidenced in core depth. No direct interaction between arsenic, iron and manganese cycle has been observed in the pore waters. The behaviour of As is mainly linked to the cycle of sulfur, and especially to the production of sulfides. Overall, this study confirms that the experimental determination of redox speciation is still very useful to understand the behaviour of As during early stages of diagenesis, since application of thermodynamic modelling to redox sensitive environments is not sufficiently constrained yet to provide reliable results.

1. Introduction

Arsenic species are mainly found in the forms of arsenate [As(V)] and arsenite [As(III)] in natural waters and sediments (Gorny et al., 2015a, 2015b, 2015c, and references therein). As the solubility, mobility and toxicity of arsenic depend on its oxidation state (Dixit and Hering, 2003; Jain and Ali, 2000), determination of As speciation and transformation is essential to understand the behaviour of As in anoxic river sediments. Indeed, these environments are highly complex due to numerous biogeochemical reactions. Early diagenetic processes are directly or indirectly linked to the degradation of sedimentary organic matter by bacteria in the first centimeters of the sedimentary column. Mineralization occurs through various metabolic processes, where the organic matter serves as a reducing agent (electron donor). This oxidative process involves the transfer of electrons between oxidants (electron acceptors) from O_2, NO_3^-, Mn(III, IV) and Fe(III) (hydr)-oxides, and finally SO_4^{2-} (Berner, 1980). Redox transformations of these major species, combined with other bacterial processes, *i.e.*, methylation, are capable to deeply modify the speciation and the fate of arsenic within the first centimeters of the sedimentary column, as well as its potential toxicity toward the aquatic organisms (Borch et al., 2009; Gorny et al., 2015a; Páez-Espino et al., 2009).

In the mineral particles, arsenic is usually found in association with aluminum, iron and manganese (hydr)-oxides, carbonates, and sulfide minerals (Drahota et al., 2009; Sadiq, 1995), with various degree of mobility. In particular, sorption processes play an important role on the control of As speciation and mobility (Bowell, 1994; Dixit and Hering, 2003). In the literature, most of the studies that focused on the sorption mechanisms were based on the examination of arsenic fractional distribution (Keon et al., 2001; Wenzel et al., 2001), the identification of As species associated with the exchangeable fraction in the solid phase (Orero Iserte et al., 2004), or the specific interaction between arsenic species and minerals (Wang and Mulligan, 2008). However, the number of experimental studies dedicated to the behaviour of As species with time and depth in pore waters remain scarce (Chaillou et al., 2003; Couture et al., 2010; Deng et al., 2014; Fabian et al., 2003).

This study aims to improve the understanding of As behaviour under the redox constraints induced within surface river sediments that

* Corresponding author.
E-mail address: Gabriel.billon@univ-lille1.fr (G. Billon).

https://doi.org/10.1016/j.gexplo.2018.01.021
Received 22 July 2016; Received in revised form 17 November 2017; Accepted 25 January 2018

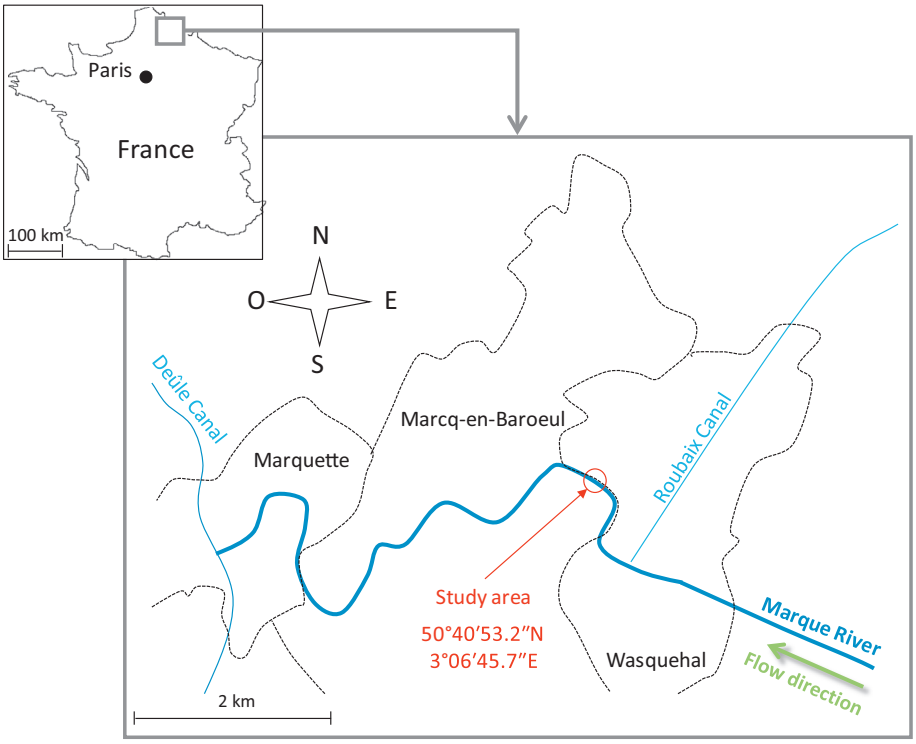

Fig. 1. Localization of the Marque River.

contain large amounts of biodegradable organic matter. For this purpose, the distribution of both As and other key elements (such as Fe, Mn and S) that potentially control the fate of As was studied in the sediment solid phase of the Marque River through sequential extractions. In addition, analyses of pore waters were performed by HPIC-ICP-MS to assess As speciation. The use of redox potential values will also be discussed to demonstrate that thermodynamic equilibrium modelling is inadequate when redox speciation is involved, and to point out the limits of geochemical modelling in such complex environments.

2. Materials and methods

2.1. Location and sampling

The Marque River, located in Northern France, was chosen as the sampling site (Fig. 1). The river rises at Mons-en-Pévèle. The watershed area is about 217 km^2 with an average slope gradient of 0.1%. The stream runs firstly through a suburban basin (down to Villeneuve d'Ascq), then it goes through an urban basin before it drains to the Deûle River at Marquette-Lez-Lille. The last 7.6 km are channelized but not navigated anymore. The River is characterized by a low flow rate of 1.0 $m^3 s^{-1}$ in average at Forest-sur-Marque, which can reach up to 5.4 $m^3 s^{-1}$ during flood events (Ivanovsky et al., 2016).

Four sampling campaigns were carried out in February, April, July and October 2014 at Marcq-en-Barœul (Fig. 1) to follow various early diagenesis biogeochemical transformations at different times of the year. Four sediment cores were collected each time using a manual corer equipped with a Perspex® tube (length 35 cm, i.d. 7.5 cm).

The sample processing method is summarized in Fig. 2. The first core was sliced on site every 1–2 cm for the determination of total dissolved As content and As speciation as a function of depth. The cutting operation was done under nitrogen atmosphere in a glove box. The second core was also sliced under nitrogen atmosphere for the determination of alkalinity, Dissolved Organic Carbon (DOC), major elements (Ca, Fe, K, Mg, Mn and Na) and nutrients (NH_4^+, NO_3^-, NO_2^- and SO_4^{2-}) in the pore waters. To do that, each sediment slice was centrifuged with an X 340 Prolabo centrifuge (rotation radius: 20 cm) during 20 min at 2500 rpm in order to extract the pore waters. The samples were subsequently filtered at 0.45 µm (Sartorius syringe filter with cellulose acetate membrane) under nitrogen atmosphere. Prior to the determination of alkalinity, DOC and ions, samples were stored at −18 °C in pre-calcinated (24 h, 450 °C) glass tubes (25 mL with Teflon/silicon septum, Sterilin). Prior to determination of total As, major and minor elements, samples were acidified at 2% (v/v) with HNO_3 (Merck, 65%, suprapur), and stored in polypropylene tubes (PP, 15 mL, Falcon®) at 4 °C. For the determination of As speciation, filtered pore water samples were stored in PP tubes until calibration of HPIC-ICP-MS and determination of As speciation was done (< 3 h). The remaining raw sediments were stored under nitrogen atmosphere at −18 °C for analyses on the solid phase. The analyses in the sediment particles were only performed once time because it has been assumed that the composition of the solid phase has not evolved significantly as the sampling site remained the same and the monitoring was performed within a period of 9 months. For information, the total concentrations, the metal distributions and the reduced sulfur species concentrations have been measured in February, July and October, respectively. The third core was used for the measurement of pH and redox potential every cm within a previously holed Perspex® tube. The fourth core was used for determination of sulfides using AgI-DGT (Diffusive Gradients in Thin films; Teasdale et al., 1999). Surface water was also sampled for analyses following the same procedures, but under oxic conditions and without centrifugation.

2.2. Pore water analyses

Measurements of pH and redox potential were performed using a glass electrode (Mettler Toledo) and a platinum electrode (Mettler Toledo), respectively. Both working electrodes are combined with an Ag/AgCl ([KCl] = 3 M) reference electrode, with a potential equal to 0.22 V *versus* the Standard Hydrogen Electrode (SHE). All potential values reported in the text are expressed *versus* the SHE electrode.

Anion concentrations (NO_3^-, NO_2^-, SO_4^{2-}) were measured using a Dionex™ ion chromatography system equipped with a separation column (IonPacAG18, length 50 mm, i.d. 4 mm, coupled with IonPac

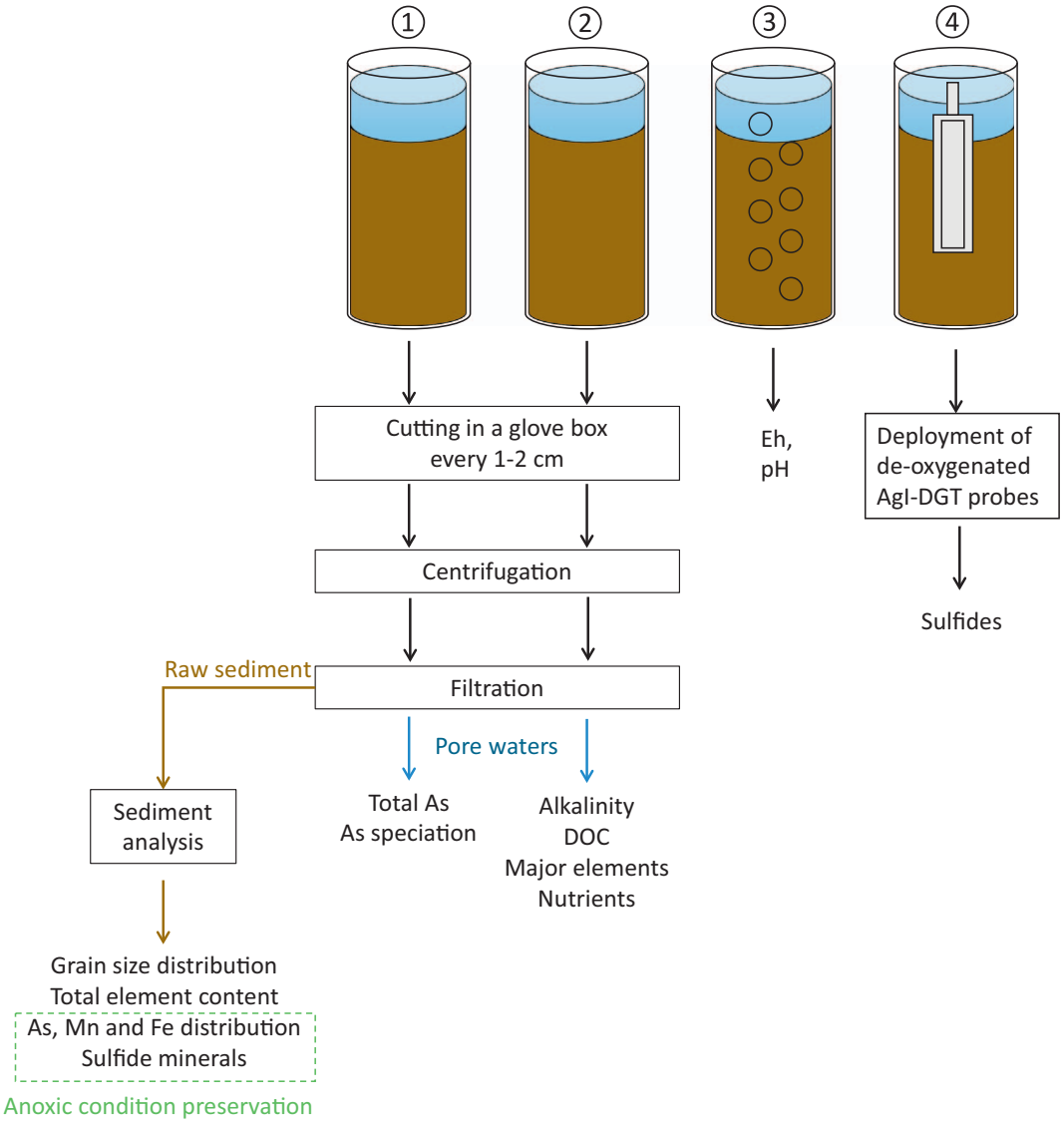

Fig. 2. Summary of the treatments applied to the sediment cores.

AS18, length 250 mm, i.d. 4 mm), a potassium hydroxide eluent generator (EG50) and an electrochemical detector (ED40).

Dissolved sulfides concentrations were measured by DGT (Diffusive Gradient in Thin film) using an AgI binding gel, the detailed preparation of which is described in Gao et al. (2009). The de-oxygenated DGT probes (under nitrogen flow for 24 h) were inserted in the sediment core for 24 h in a thermostatic chamber set to the field temperature. After deployment, each DGT probe was rinsed quickly with ultrapure water (Milli-Q, Merck Millipore) and put in a well-humidified plastic box before treatment. The sulfide concentration was determined using a flatbed scanner (300 dpi) from grey level records after calibration experiments.

Dissolved Organic Carbon (DOC) was measured with a TOC-V_{CSH} analyzer. DOC was determined using the high-temperature (900 °C) catalytic oxidation method with CO_2 IR detection (Ammann et al., 2000; Callahan et al., 2004), previously calibrated using potassium hydrogenophtalate (Shimadzu) standard solutions.

Ammonium was analyzed by spectrophotometry (Varian, Cary 300) according to the analytical procedure described by Weatherburn (1967).

Alkalinity, mainly in the form of HCO_3^-, was measured using an automatic pH titrator (Metrohm, model Titrino 736 GP) with a $5\,10^{-3}$ M HCl solution [see Lesven et al., 2008 for more details].

Metal concentrations in the pore waters were determined by Inductively Coupled Plasma – Optical Emission Spectrometry (ICP-OES; Varian Vista Pro, axial view) or by Inductively Coupled Plasma – Mass Spectrometry (ICP-MS; Thermo Elemental™ X-series) depending on the concentration levels. Arsenic speciation was assessed by coupling beetwen High Performance Ion Chromatography (HPIC; Thermo ScientificTM DionexTM ICS-5000+) and ICP-MS (see Gorny et al. (2015b) for operating conditions). Starting from 25 µL of pore waters, the different As species, *i.e.*, As(III), As(V), $MMAA^V$ (monomethyl arsenic acid), and $DMAA^V$ (dimethyl arsenic acid) were separated in < 4 min using a IonPac® AG7-AS7 anion-exchange column set and helium-purged 1 and 50 mM HNO_3 as a mobile phase. The detection limits were below or equal to 0.25 µg L^{-1}. Qualitative measurement of thio-arsenic species is possible based on the chromatographic peak area, *i.e.*, the ratio between the peak area of thio-arsenic species and the sum of the peak areas of all As species. This methodology is useful since no standard for thio-arsenic species is commercially available.

2.3. Sediment analyses

Grain size distribution was determined by laser granulometry on

wet sediment (Malvern Mastersizer 2000). In order to characterize the mineralogical composition of the sediment particles, air-dried samples and clay-size fraction were analyzed by X-ray diffraction, using a D8 advance Bruker AXS diffractometer equipped with a Cu anode (CuK_{alpha}) and a 1D LynxEye PSD detector; for more details, see Bout-Roumazeilles et al. (1999).

Total carbon and nitrogen content in dry sediment samples were determined using an elemental CHNS analyzer LECO model 932. Particulate Organic Carbon (POC) was determined by the ignition loss method; for more details, see Louriño-Cabana et al. (2011).

Amorphous iron and manganese (hydr)-oxides (and associated As) were extracted under nitrogen atmosphere from 0.4 g of wet sediment using 20 mL of ascorbate solution (pH = 8.2, $[NaHCO_3] = 0.6\ mol\ L^{-1}$, [trisodium citrate] = 0.2 M and [ascorbic acid] = 0.1 M) (Haese et al., 2000; Jones and Turki, 1997; Kostka et al., 1995).

Reactive fraction ($M_{reactive}$) of Fe and Mn (*i.e.*, mainly exchangeable, bound to organic matter, amorphous and poorly-crystallized (hydr)-oxides, calcite, phosphate and AVS) were extracted under nitrogen atmosphere from 2 g of wet sediments and 20 mL of 1 M HCl solution during 24 h (Canfield, 1988; Chao and Zhou, 1983; Cooper and Morse, 1998; Kostka and Luther, 1994). It is therefore possible to evaluate by calculations the fractionation of Fe and Mn through: (i) reducible (hydr)-oxides (ascorbate reactive concentrations), (ii) exchangeable fraction without reducible (hydr)-oxides (HCl reactive concentration *minus* ascorbate reactive concentration), and (iii) residual fraction (total concentration *minus* HCl reactive concentration), *i.e.*, detrital aluminosilicate minerals, refractory oxides, organic matter and sulfides.

Acid Volatile Sulfur (AVS) and Chromium Reducible Sulfur (CRS) were evaluated by potentiometry after their conversions into H_2S gas following the experimental procedure described by Billon et al. (2001). Determination of AVS, CRS and reactive iron ($Fe_{reactive}$, obtained by extraction using HCl 1 M at room temperature for 24 h) allows for the calculation of the degree of sulfidization (DOS) and the degree of pyritization (DOP) (Gagnon et al., 1995):

$$DOS = \frac{[Fe_{CRS}] + [Fe_{AVS}]}{[Fe_{CRS}] + [Fe_{reactive}]} \quad (1)$$

$$DOP = \frac{[Fe_{CRS}]}{[Fe_{CRS}] + [Fe_{reactive}]} \quad (2)$$

where $[Fe_{AVS}]$ and $[Fe_{CRS}]$ are the amounts of iron bound to AVS (considering that the main precipitate is FeS) and CRS (considering that the main precipitate is FeS_2), respectively.

Total element contents, *i.e.*, Al, Ca, Fe, K, Mg, and Mn, were determined after total mineralization on dry samples using a mixture of nitric and hydrofluoric acids, and aqua regia, following the protocol of Boughriet et al. (2007).

Fractionation of arsenic in wet sediments was done using the modified sequential extraction procedure proposed by Ruban et al. (2001). The method gives access to three groups of sedimentary solid fractions: (i) exchangeable fraction (NaOH 1 M); (ii) internalized reactive fraction (HCl 1 M); and finally (iii) residual fraction (acid mineralization previously described for total element content). The two first steps were performed under nitrogen atmosphere. No speciation measurement was performed on the NaOH exchangeable fraction: acid-base reaction would occur between mobile phase (dilute HNO_3) and extracting solution (NaOH 1 M) that would modify chromatographic conditions for separating As species.

Total element concentrations in extracts were analyzed by ICP-OES or ICP-MS depending on the concentration. Spectrometers were calibrated using standard solutions (with a minimum acceptable $R^2 > 0.995$), blank correction was applied when necessary, and standard reference materials were analyzed regularly to control the analysis quality. Results of control analysis quality are presented Table S1 with correct extraction yields (> 80%).

2.4. Geochemical modelling

Visual Minteq v3.00 (Gustafsson, 1991) was used to calculate the speciation of pore waters assuming that thermodynamic equilibrium is reached. The software was also used to predict some possible precipitation/dissolution reactions through the calculation of the saturation indexes. Input data are the concentrations of the following components in the pore waters, *i.e.*, As(III), As(V), Ca^{2+}, Cl^-, DOC, Fe^{2+}, K^+, Mg^{2+}, Mn^{2+}, Na^+, NH_4^+, NO_3^-, NO_2^-, SO_4^{2-}, and HS^-. The redox potentials measured with the platinum electrode, Eh, were not considered in the calculations since their values did not verify the assumption of thermodynamic equilibrium (see part 3.4.2). Other parameters were also considered, *i.e.*, alkalinity, ionic strength, pH and temperature. Finally, the output file described the predicted speciation of each component in pore waters and saturation index (Ω) with respect to any mineral phase. Hence, pore water is considered as supersaturated with respect to a mineral for $\Omega > 0$, at equilibrium for $\Omega = 0$ and undersaturated for $\Omega < 0$.

3. Results and discussion

3.1. General composition of the sediments

The average concentrations in the sediments are presented in Table 1. The results exhibit only slight and similar relative changes for major and minor elements throughout the core (RSD < 25%, n = 12). The average concentrations of Al, Fe and Mn are very close to those recorded from deep horizons in Northern France. These relative constant profiles suggest a common source for all these elements with no real change of particle composition. Al, K, Fe and Mg concentrations are generally well-correlated ($R^2 > 0.82$), which corresponds to the elemental signature of terrigenous fine particles like clays (Li and Schoonmaker, 2003; Luoma et al., 2008). This assumption is reinforced by the granulometric analyses (Fig. 3), which show that the sediment contains 85% fine grain particles (size < 63 μm). Mineralogical analysis of the clay fraction (size < 2 μm) reveals the main presence of smectite (62.5%), and to a lesser extent of illite (22.5%), kaolinite (10%), and chlorite (5%). Mineralogical analyses were also carried out on the fine fraction (< 63 μm) of the sediment. Quartz is the major constituent of the solid phase, followed by calcite (0.6%), and to a lesser extent by clays.

The contamination of As in the sediments was evaluated by considering the enrichment factor (EF) as defined previously (Atteia, 1994):

Table 1
Average elementary composition of sediment particles from the Marque River and soil horizons from Nord-Pas de Calais loess deposits (Sterckeman et al., 2006).

	Al	As	Ca	C	Fe	K	Mg	Mn	N
	$g\ kg^{-1}$	$mg\ kg^{-1}$	$g\ kg^{-1}$	$g\ kg^{-1}$	$g\ kg^{-1}$	$g\ kg^{-1}$	$g\ kg^{-1}$	$mg\ kg^{-1}$	$g\ kg^{-1}$
Mean value	58	11	27	60	37	17.5	8	400	5.5
RSD (%)	8	20	9	15	12	5	10	12	21
Regional values from deep horizons	50.3	10			27.4			427	

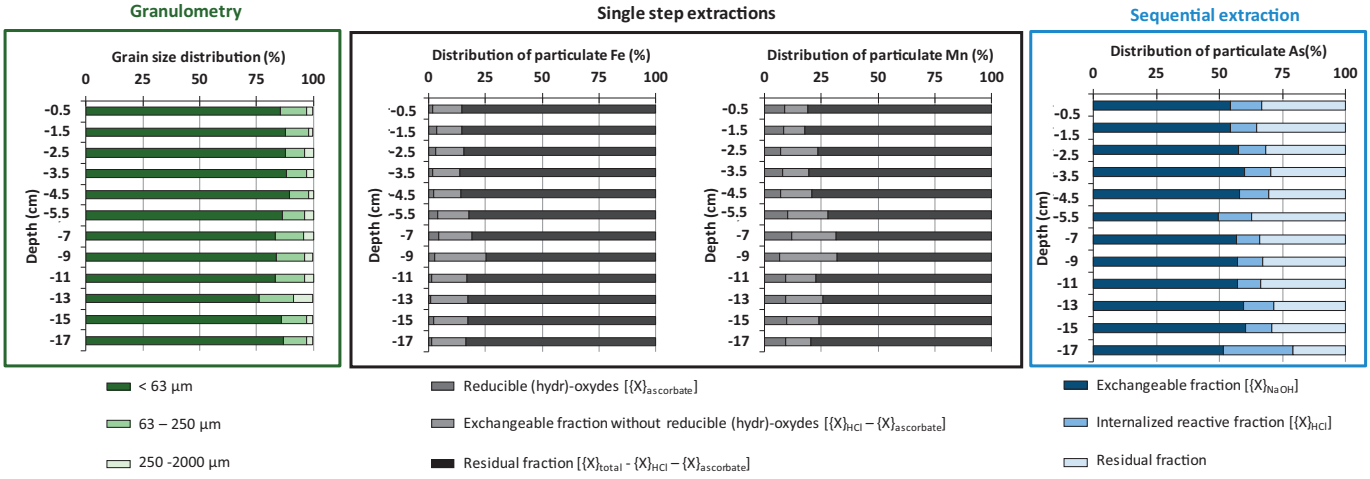

Fig. 3. Depth profiles of grain size distribution, and As, Fe and Mn distribution in the solid phases.

$$EF_{Al}^{As} = \frac{\left(\frac{[As]}{[Al]}\right)_{sample}}{\left(\frac{[As]}{[Al]}\right)_{reference}} \quad (3)$$

with [As] and [Al] the total amount of As and Al. For that purpose, the following background concentrations were used, *i.e.*, $[As]_{background} = 10.0\ mg\ kg^{-1}$ and $[Al]_{background}$ $50.3\ g\ kg^{-1}$, respectively [average composition of soil horizon from Nord-Pas de Calais loess deposits, see Sterckeman et al. (2006) and Sterckeman et al. (2002)]. In the Marque river sediments, the average value of EF_{As} is 0.95, clearly indicating that the site is not contaminated with As. In addition, the concentration variation as a function of the depth is very limited, with a RSD < 15% for 12 values (Table 1).

3.2. Distribution of particulate Fe, Mn and S

According to Gorny et al. (2015a, 2015b, 2015c), several elements, including mainly Fe, Mn and S, control at least partly the redox behaviour of As in surface sediments during early diagenetic processes. The distribution of these elements in the solid phase is also closely examined in this section.

Iron is mainly associated to the residual fraction (83% with a RSD of 5%) in all the cores (Fig. 3). Only a small proportion in the residual fraction was found as pyritic compounds (average value of 1% calculated from $Fe_{CRS} / Fe_{residual}$). In the reactive fraction, iron is significantly associated with mono-sulfide minerals (average value of 24% calculated from $Fe_{AVS} / Fe_{reactive}$). Conversely, only a small amount of amorphous iron(III) (hydr)-oxides (2.5%) is detected whatever the depth. Iron distribution can be explained as follows: (i) production of HS^-, CO_3^{2-}, PO_4^{3-} is not sufficient to impact the iron speciation as depth profiles generally remain constant; and/or (ii) iron transformation occurs in the first millimeters of the cores and variations are not visible at our scale of observation. This last assumption is supported by the presence of AVS in the surface sediments ($1.3\ g\ S\ kg^{-1}$), meaning that both sulfates and iron (III) reducing processes occur close to the water-sediment interface.

Distribution of manganese in the solid phase differs from that of iron (Fig. 3). Compared with Fe, Mn is indeed less associated with the residual fraction (76% with a RSD of 5%), as well as with the carbonate, phosphate, and mono-sulfide minerals, and/or Particulate Organic Matter (POM) (9%). In the reactive fraction, rhodochrosite ($Mn^{II}CO_3$) appears from thermodynamic equilibrium calculation to be the most likely mineral assemblage (median $\Omega > 0.55$, Table 2). The proportion of amorphous $Mn^{III,IV}$-hydroxides is higher (15%) than iron-hydroxides. Nevertheless, changes of the redox properties during early diagenesis do not appear to strongly impact the distribution of particulate manganese.

AVS and CRS profiles are displayed in Fig. 4. The concentrations of these reduced sulfur species are already significant close to the water-sediment interface. Indeed, sulfidization processes are active from the first millimeters of the cores as confirmed by the concentration profiles of dissolved sulfates (Fig. 4). Sulfate consumption occurs mainly close to the water-sediment interface when compared to the values measured in the overlying water (from $100\ mg\ L^{-1}$ to $< 10\ mg\ L^{-1}$ below 0.5 cm depth). Therefore, it is likely assumed that the production of sulfides is limited to the sulfate inputs. Sulfidization and pyritization mechanisms are not complete (DOS ~ 43% and DOP ~ 10%), as already supported by the speciation of the particulate iron. Small amount of (hydr)-oxides is indeed present all along the cores (Fig. 3). Similar results have been found in the surrounding rivers with DOS and DOP values, which do not exceed 70 and 25%, respectively (Lesven, 2008; Prygiel, 2013).

3.3. Distribution of particulate arsenic

The distribution of arsenic in the cores is relatively homogenous with depth (RSD < 25%, Fig. 3): the exchangeable fraction reaches 57% while the residual fraction is 31% and the fraction associated to carbonates, (hydr)-oxides, phosphate and/or mono-sulfide minerals (also called internalized reactive fraction) is 12%. These results suggest that an important fraction of arsenic is easily available in the sediments of the Marque River. Although the NaOH solution used to extract the exchangeable As is also capable to dissolve orpiment (As_2S_3) (Floroiu et al., 2004) contrary to iron sulfides (Rickard, 2006), orpiment is unlikely to be present in the sediment ($\Omega \ll 0$, Table 2). In the pH range (from 6.5 to 8) of the Marque River pore waters, chlorite, illite, kaolinite and quartz are not relevant adsorbent phases for As species since these minerals are generally characterized by pH_{PZC} values < 5 (Alvarez-Ayuso and Garcia-Sanchez, 2003; Besra et al., 2000; Hussain et al., 1996; Singh et al., 1996). Adsorbent mineral phases for As species are rather aluminum (hydr)-oxides (pH_{PZC} = 7.5–8.5) (Álvarez-Ayuso et al., 2007; Hongxia et al., 2005), amorphous iron and manganese (hydr)-oxides (pH_{PZC} = 6.3–9.1) (Appelo et al., 2002; Marmier et al., 1999; Wilk et al., 2005; Zaman et al., 2009) and calcite (pH_{PZC} = 8.2–9.5) (Churchill et al., 2004; Salinas-Nolasco et al., 2004). The residual fraction contains a significant amount of As, suggesting interactions with CRS and/or POM. However, no significant correlation was evidenced between CRS and residual As. However, it is not surprising since most of the sulfidization processes occur in the first mm below the water-sediment interface. The internalized reactive fraction corresponds to As species internalized in reactive mineral phases through co-precipitation processes (Alexandratos et al., 2007; Bose and Sharma, 2002). Amorphous iron (hydr)-oxides can be relevant of

Table 2
Saturation index for carbonate, oxide and sulfide minerals in pore waters in 2014. Temporal evolution of the saturation indexes for each campaign is also available in supporting information (Table S2). Solubility products (Ksp) used for saturation index calculations are provided in the database of Visual Minteq.

	Calcite	Disordered dolomite	Ordered dolomite	Magnesite	Siderite	Rhodochrosite	Amorphous iron-monosulfide	Mackinawite	Green manganese mono-sulfide	Pink manganese mono-sulfide	Pentoxide arsenic	Orpiment	Claudetite	Arsenolite
	$CaCO_3$	$CaMg(CO_3)_2$	$CaMg(CO_3)_3$	$MgCO_3$	$FeCO_3$	$MnCO_3$	FeS	FeS	MnS	MnS	As_2O_5	As_2S_3	As_2O_3	As_2O_4
Average	0.81	0.52	1.07	−0.89	0.65	0.49	−0.93	−0.28	−4.43	−7.43	−38.29	−10.46	−14.22	−14.18
Median	0.80	0.56	1.11	−0.87	0.78	0.55	−0.59	0.06	−4.03	−7.03	−35.79	−10.04	−14.51	−14.47
Standard deviation	0.27	0.51	0.51	0.25	0.90	0.37	1.99	1.99	1.78	1.78	5.87	5.32	1.02	1.02
Minimal	0.30	0.39	0.16	−1.42	−1.38	−0.34	−12.56	−11.91	−14.71	−17.71	−51.80	−39.01	−15.84	−15.80
Maximal	1.34	1.47	2.02	−0.47	2.02	1.22	0.48	1.13	−3.39	−6.39	−33.55	−6.49	−12.45	−12.41
K_{sp}	−8.41	−16.11	−16.72	−2.85	−10.80	−10.98	−2.95	−3.60	−0.02	2.98	−61.95	−46.30	−1.34	−1.38

mineral phases as pointed out through the extraction with the ascorbate solution ($R^2 = 0.91$).

3.4. Diagenetic tracers

3.4.1. Eh and pH profiles

Recorded Eh and pH profiles are typical of a system in which early diagenetic processes occur (Fig. 5). Pore waters are more acidic (pH ~ 7) than the overlying waters (pH ~ 8). A gradual decrease in pH is observed with depth, down to a value of 6.75–7 below 10 cm. Acidification of pore waters is linked to a set of chemical reactions *e.g.*, aerobic respiration and sulfato-reduction that dominate, in these sediments, over the release of hydroxide ions [such as precipitation of iron mono-sulfide, reduction of manganese (hydr)-oxides by Fe(II)] (Metzger, 2004). Whatever the sampling campaign, the redox potential values (Eh *vs* SHE) range from +150 to +600 mV in overlying water. The redox conditions are stabilized below 2 cm in depth but are more reductive with the seasons: +30 mV in February, −36 mV in April, −29 mV in July, and −65 mV in October. These profiles clearly indicate that: (i) the consumption of oxidants by bacteria during the diagenetic processes is important at the water-sediment interface; and (ii) the sediment becomes rapidly anoxic with no real significant evolution of the redox properties below 2 cm in depth.

3.4.2. Eh vs redox couples

The meaning of the redox potential values has been evaluated through a mechanistic approach that determines all the relevant redox couples which are susceptible to affect the Eh values measured by the Pt electrode (Billon et al., 2005; Stefánsson et al., 2005). The activity of each redox species given by Visual Minteq is presented in Table 3. Calculations of equilibrium potentials (E_{eq}) were performed using the Nernst-equation using the couples capable to control the redox potential in the sediments. Results are presented in Fig. 6. Slight variations in the range of E_{eq} are observed between the 4 campaigns. Comparison of E_{eq} with the standard potential ($E_{pH\approx7.5}{}^0$) provides qualitative information about the abundance of oxidized and reduced species for each redox couple considered. Oxidized species predominate for Fe (III)/Fe(II), Mn(III,IV)/Mn(II) and S^0/H_2S couples since $E_{eq} > E_{pH\approx7.5}{}^0$, which is consistent with the existence of both Fe(III) and Mn(III,IV) (hydr)-oxides in the sediments, and with the low concentrations of dissolved Fe(II), Mn(II) and S(-II) in the pore waters. In addition, the proportion of reduced and oxidized species is approximately the same ($E_{eq} \sim E_{pH\approx7,\ 5}{}^0$) for NO_3^-/NO_2^-, NO_3^-/NH_4^+ and SO_4^{2-}/HS^- couples. Eh values measured with the Pt electrode in the first 2 cm of depth can be also thermodynamically linked to several redox couples, *i.e.*, Fe(III)/Fe(II), Mn(III, IV)/Mn(II), NO_3^-/NO_2^-, NO_3^-/NH_4^+, S^0/H_2S. However, the redox couples of nitrogen, manganiferous and sulfur species do not control the Eh because the electron transfer at the Pt electrode is too slow to reduce or oxidize these species. The associated charge transfer resistance is therefore so high that these redox couples can be considered as electrochemically inactive (Héduit, 1989; Meyer et al., 2014; Peiffer et al., 1992; Stefánsson et al., 2005; Vershinin and Rozanov, 1983). Consequently, in these anoxic environments, Eh measurements in sediments must be considered only as qualitative indicators of the reduction of Fe(III) (hydr)-oxides. Finally, integrating the Eh values in a thermodynamic model does not appear relevant to evaluate the speciation of redox sensitive elements in subsurface environments: (i) redox reactions are normally not at chemical equilibrium because electron transfer reactions are usually kinetically slow; (ii) non-ideal behaviour of the Pt electrode is observed, particularly when this last one is affected by the presence of surface coatings; (iii) some redox reactions are not reversible as they are microbial mediated; and (iv) most environmental systems have low concentrations of redox elements and thus exchange currents on the electrode surface are often too low to establish a reliable potential (Eh) (Meyer et al., 2014). It seems more accurate to determine experimentally the

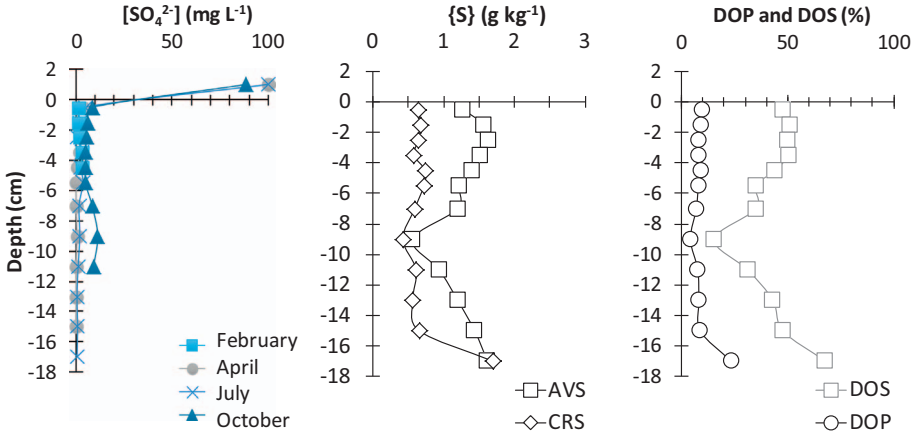

Fig. 4. Depth profiles of dissolved sulfate concentration in pore waters, and of Acid Volatile Sufides (AVS), Chromium Reducible Sulfur (CRS), total sulfur content, degree of sulfidization (DOS) and degree of pyritization (DOP) in particulate phase.

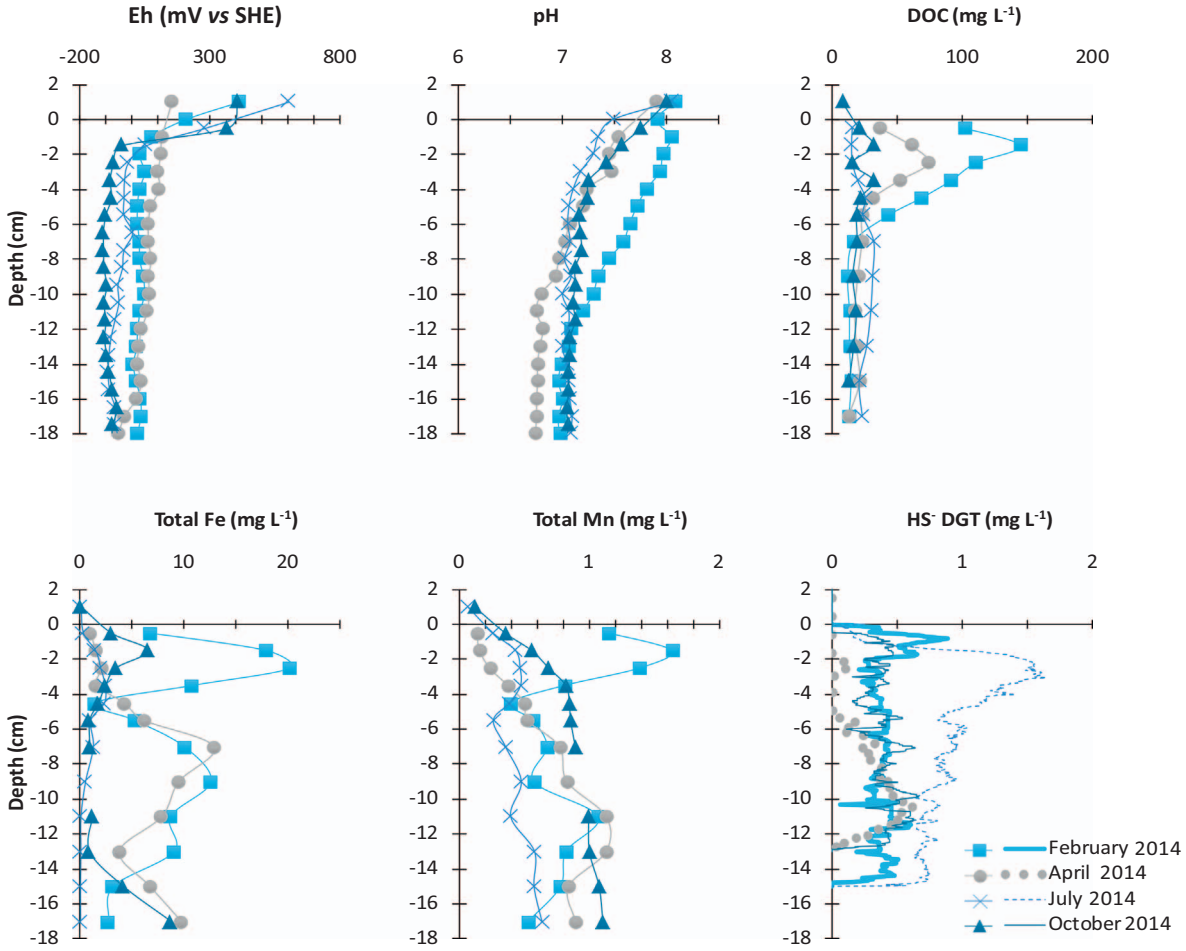

Fig. 5. Seasonal variations of pH, Eh, Dissolved Organic Carbon (DOC), total Fe and Mn content and sulfides (only free and/or labile fraction) with depth in pore waters from sediment cored in the Marque River in February, April, July and October 2014.

speciation rather than using thermodynamic modelling to better understand the fate of redox sensitive species.

3.4.3. Carbon species

Depth profiles of alkalinity are not sensitively different over time, and its average concentration is about 0.12 mol L^{-1} (RSD < 35%). As predicted, the concentrations of hydrogenocarbonates are higher in pore waters than in the overlying waters due to the mineralization of the organic matter. The highest concentrations of Dissolved Organic Carbon (DOC) (40–140 mg L^{-1}) are found in the first 6 cm, especially during winter and spring. DOC probably originates either from urban inputs of dissolved organic matter or from the decomposition of POM of terrigenous origin, which concentration is higher during fall (Sun and Dai, 2005). Carbonate production in pore waters during mineralization of POM can regulate the concentration of some cationic metals, *i.e.*, Ca^{2+}, Fe^{2+}, Mn^{2+} and Mg^{2+}. The saturation indexes of pore waters as calculated with Visual Minteq are presented in Table 2. Supersaturated minerals are calcite [$CaCO_3$] (observed by XRD), dolomite [$CaMg(CO_3)_2$], siderite [$Fe^{II}CO_3$], and rhodochrosite [$Mn^{II}CO_3$] with median $\Omega > 0.55$. It is unlikely to observe magnesite [$MgCO_3$] in the

Table 3
Standard potentials ($E_{pH=0}^{0}$) and standard potentials corrected to pH 7.5 ($E_{pH=7.5}^{0}$) of some electrochemical couples presumed to be potentially active in the sedimentary environment. References: Billon et al. (2005) (a) and Meyer et al. (2014) (b).

Redox equations	$E_{pH=0}^{0}$ (mV)	$E_{pH=7.5}^{0}$ (mV)	References
$FeOOH\ (s) + 3H^+ + e^- \leftrightarrow Fe^{2+} + 2\ H_2O$	+1080	−248	a
$Fe(OH)_3\ (s) + 3H^+ + e^- \leftrightarrow Fe^{2+} + 3\ H_2O$	+1015	−312	a
α-$FeOOH$ (goethite) $+ 3H^+ + 1\ e^- \leftrightarrow Fe^{2+} + 2\ H_2O$	+804	−524	a
α-Fe_2O_3 (hematite) $+ 6H^+ + 2\ e^- \leftrightarrow 2\ Fe^{2+} + 3\ H_2O$	+790	−538	a
Fe_3O_4 (magnetite) $+ 8H^+ + 2\ e^- \leftrightarrow 3\ Fe^{2+} + 4\ H_2O$	+1097	−673	a
$MnOOH$ (manganite) $+ 3H^+ + e^- \leftrightarrow Mn^{2+} + 2\ H_2O$	+1050	−278	a
Mn_3O_4 (hausmanite) $+ 8H^+ + 2\ e^- \leftrightarrow 3\ Mn^{2+} + 4\ H_2O$	+1823	+53	a
MnO_2 (manganate) $+ 4H^+ + 2\ e^- \leftrightarrow Mn^{2+} + 2\ H_2O$	+1292	+407	a
MnO_2 (pyrolusite) $+ 4H^+ + 2\ e^- \leftrightarrow Mn^{2+} + 2\ H_2O$	+1229	+344	a
$NO_3^- + H_2O + 2\ e^- \leftrightarrow NO_2^- + 2\ OH^-$	+17	+400	b
$NO_3^- + 10H^+ + 8\ e^- \leftrightarrow NH_4^+ + 3\ H_2O$	+274	+327	b
$SO_4^{2-} + 5\ H_2O + 8\ e^- \leftrightarrow HS^- + 9\ OH^-$	−683	−251	b
$S^0\ (s) + 2H^+ + 2\ e^- \leftrightarrow H_2S$	+144	−299	b

particulate phase ($\Omega < -0.87$). Previous studies have shown that As (V) adsorbs readily on calcite (Sø et al., 2008), calcite-containing material (Romero et al., 2004; Yolcubal and Akyol, 2008) and dolomite (Ayoub and Mehawej, 2007; Salameh et al., 2010). Conversely, As(III) retention is known to be very limited on calcite (Sø et al., 2008; Yokoyama et al., 2009; Yokoyama et al., 2012) (no data exist on dolomite). It has also been shown that As(V) adsorbs onto siderite up to pH 8 (Jönsson and Sherman, 2008) and iron (hydr)-oxides (Dixit and Hering, 2003; Xu et al., 1991). These data suggest that dissolved As(III) should be the dominant species in the sediments of the Marque River, as carbonate minerals are relatively abundant to sorb As(V).

3.4.4. Nitrogen species

Depth profiles of NO_3^- are similar whatever the sampling period (Fig. S1). Both concentrations drastically decrease in the first mm of the sediment core (over 90%). This observation suggests a rapid consumption of nitrates at the water-sediment interface, probably concomitant to the oxygen disappearance. Depth profiles of NH_4^+ are relatively similar between February and July (Fig. S1). Concentrations gradually increase with the depth, up to 55 mg L^{-1}. In October, concentrations are higher in the first 8 cm of sediment with a maximum at −6 cm (70 mg L^{-1}).

3.4.5. Sulfur species

Sulfate-reducing bacteria are active in sediments of the Marque River. They rapidly consume 96% of sulfates just below the water/sediment interface (Fig. 4) (Roosa, 2013; Nealson, 1997). The sulfide production fluctuates according to the sampling period. It is more intense in July, with an average concentration of dissolved sulfide of 860 µg L^{-1} (Fig. 5). The increase of the bacterial activity during the summer is typical of sulfate-reducing bacteria in river sediments (Grabowski et al., 2001). Regarding Mn, MnS precipitation cannot happen, as median $\Omega < 0$ (Fig. 4). According to Morse and Luther III (1999), manganese would rather be associated with pyrite ($Fe^{II}S_2$) when DOP values are above 40%, which is not the case here (4–23%). It is likely that the sulfides do not control the behaviour of Mn in the sediments. Conversely, the presence of iron sulfides is clearly evidenced whatever the depth and the sampling period. It is therefore not surprising that saturation index values of FeS are close to saturation ($-0.59 <$ median $\Omega < 0.06$). Previous studies have shown that sulfide minerals efficiently trap inorganic species (Bostick and Fendorf, 2003; Han et al., 2013) and As(V) species (Wolthers et al., 2005). This still suggests that As(III) must be relatively more mobile than As(V) in the sulfidic sediments of the Marque River.

3.4.6. Iron and manganese

Concentration profiles of Fe and Mn are very different according to the sampling period (Fig. 5). For Fe, three reductive and/or dissolution zones have been evidenced. The first one is located between 0 and −4 cm, where intense mineralization of organic matter should occur, accompanied by the reduction of Fe(III). Iron concentration is the highest in February (20 mg L^{-1}), and falls drastically from April (close to 2 mg L^{-1}) to finally increase again in October (6.7 mg L^{-1}). The second production of dissolved Fe(II) is located between −4 and

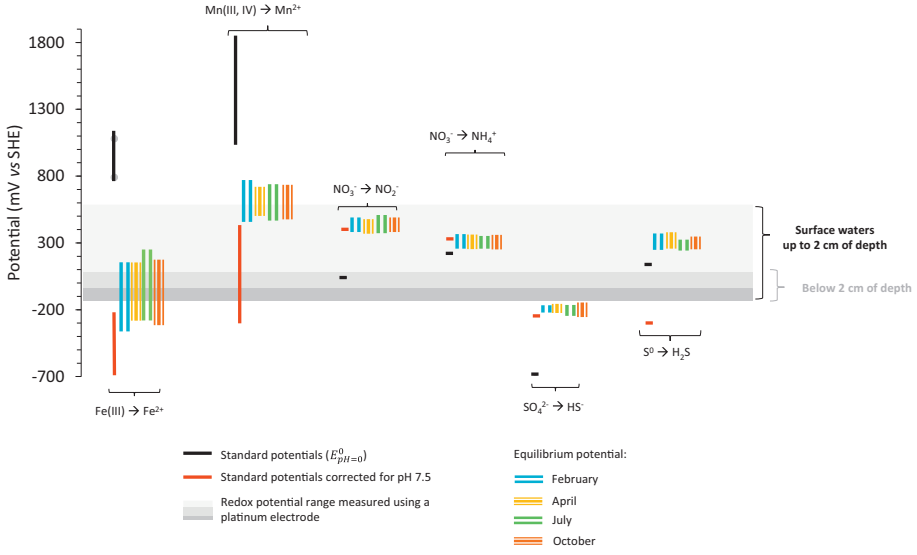

Fig. 6. Comparison between the natural redox potentials measured in the sediment samples with a platinum electrode (*vs* SHE) and the potentials corresponding to redox couples involving iron, manganese, nitrogen and sulfur.

−14 cm in depth, where Fe concentration reaches a maximum of 13 mg L^{-1} in February and April. The last zone of production of dissolved iron is localized below 14 cm in depth, where maximal concentrations are recorded in April and October (9 mg L^{-1}). Unfortunately, dissolution remains unexplained in the two deepest zones, with neither higher DOC concentrations nor lower pH values.

Regarding Mn, a gradual increase of concentrations over the first 8–10 cm in depth is noticed (except in February where a strong reductive dissolution is observed at −2 cm). From a thermodynamic point of view, the profiles of Mn and Fe are unusual. The production of Mn(II) is indeed usually recorded before the appearance of dissolved Fe (II) (Jørgensen, 2006; Schulz and Zabel, 2006). However, in the sampling site, several early diagenetic processes, including oxygen consumption, denitrification, and sulfide production, simultaneously occur just below the water-sediment interface. These processes are likely due to the presence of an important stock of biodegradable organic matter. The solubility of iron and manganese in the pore water also depends partly on the carbonate (Jensen et al., 2002), sulfide (Morse and Luther III, 1999) and dissolved organic matter concentrations (Charriau et al., 2011). In the case of the Marque River sediments, there is no doubt that reduced sulfur species impact the solubility of dissolved iron(II) due to the presence of amorphous sulfides ($Fe^{II}S$; ~1.3 g kg^{-1} of AVS), pyrite ($Fe^{II}S_2$; ~0.7 g kg^{-1} of CRS). From a thermodynamic point of view, it is possible that carbonates species also influence the solubility of dissolved iron(II) and manganese(II) by the formation of carbonate minerals (median Ω ~ 0.78 and ~0.55 for $Fe^{II}CO_3$ and $Mn^{II}CO_3$, respectively).

As demonstrated in the section related to carbon and sulfur species, the concentrations of dissolved iron and manganese are likely controlled by the precipitation of several mineral phases of amorphous sulfides ($Fe^{II}S$; ~1.3 g kg^{-1} of AVS), pyrite ($Fe^{II}S_2$; ~0.7 g kg^{-1} of CRS), siderite ($Fe^{II}CO_3$; median Ω ~ 0.78) and/or rhodochrosite ($Mn^{II}CO_3$; median ~0.55).

Overall, diagenetic tracers show clearly an obvious reduction of the main oxidants in the first centimeters of the sediment. From these results, the behaviour of dissolved As in terms of concentration and speciation is going to be examined in the last section.

3.5. Behaviour of arsenic and speciation in pore waters

The total concentrations as well as the speciation of arsenic in pore waters significantly changes with time (Fig. 7). In February, the highest total As concentration (10 µg L^{-1}) is recorded at the water-sediment interface. Then, it gradually decreases with depth, down to 2 µg L^{-1}. As (III) is the dominant species whatever the depth, with a maximum value at the water-sediment interface (90%). These results indicate that the reduction of As(V) happens before the reduction of manganese and iron (hydr)-oxides (maximal concentrations for total dissolved Mn and Fe at −2 and −3 cm, respectively). It also suggests that the redox reactive As (V) should be mostly adsorbed onto particles rather than internalized in any mineral structure. As(V) can be directly reduced on minerals by sulfides, leading to a release of dissolved As(III). As(V) is hardly detected above 8 cm in depth with concentrations close to the detection limit (0.05 µg L^{-1}). The overall proportion of As(V) represents < 10% of the total As concentration, confirming that the sedimentary column is really anoxic. The second zone of the iron dissolution (observed between 6 and 14 cm in depth) does not result in the remobilization of As (V) and/or As (III) in interstitial waters, suggesting that most of As(V) has been already reduced in the surface sediments, and that the behaviour of iron and arsenic is not so interconnected in these sediments. Below 6 cm in depth, pore waters are characterized by a significant presence of thio-arsenic species (30–70%, as measured by HPIC-ICP-MS), which allows for a stabilization of As(III) in solution. Although sulfides and As(III) are together present in the surface sediments, the production of thio-arsenic species should be kinetically slow (Rochette et al., 2000; Zhang et al., 2014).

In April, two maxima were observed at −1.5 and −11 cm (6 and 10 µg L^{-1}, respectively). The evolution of As speciation as a function of depth is less conventional than in February. Intense variations in the proportion of As(III) and As(V) are indeed observed in the first 10 cm of the core. As(V) becomes the main dissolved As species below 10 cm in depth, with a proportion reaching 90%. The thio-arsenic species were found to represent only a minor fraction of the dissolved As species with an average proportion of 10% throughout the core. As the least negative redox potential values are observed in April (Fig. 5), it is proposed that less efficient reduction of As(V) to As(III) at that time may be due to resuspension events and/or bioturbation processes. The stability of As (V) was also accompanied by low concentrations of sulfides, especially within the 6 first cm. It is also possible that advective flow of groundwater carried oxidizing agents into the sediments during sampling, resulting in a decrease of the dissolved sulfide concentration and a release of As(V) co-precipitates.

The depth profiles of As(III) and total As are well correlated in July (R^2 ~ 0,8) with an increase in the first 6 cm (at a depth of 6 cm, $[As]_{total}$ = 8 µg L^{-1}), before a global drop with some fluctuations is recorded. Like in February, As(V) concentrations are low and, in this particular case, even not detected ([As] < 0.1 µg L^{-1}). As speciation is divided into As(III) (80%) and thioarsenic species (20%) all along the core. This characteristic is bound to the highest production of dissolved sulfides with a peak production of 1.6 µmol L^{-1} at −3 cm in depth.

The lowest concentrations of total As were measured in October, with a maximum concentration of only 3.4 µg L^{-1}. This is probably related to a decrease of sulfate-reducing bacteria compared to July. No quantitative speciation can be obtained below 3.5 cm of depth as the values are lower than the detection limit (0.25 µg L^{-1}). As(III) remains the main dissolved As species in pore waters. The concentration is maximal at −0.5 cm, just above the zone where the reductive dissolution of iron (hydr)-oxide occurs. Then it gradually decreases with depth.

From thermodynamic equilibrium calculations, precipitation of arsenic pentoxide ($As^{V}_2O_5$), arsenolite ($As^{III}_2O_3$), claudelite ($As^{III}_2O_3$) and orpiment ($As^{III}_2S_3$) cannot be possible because Ω < 0 (Table 2). These results rather suggest that the solubility of dissolved As(III) and As(V) in pore waters should be regulated by the sorption on some mineral phase, As being mainly associated to the exchangeable fraction. Several mineral hosts can be responsible for As sorption onto the sediments of the Marque River, like amorphous iron and manganese (hydr)-oxides, calcite and siderite ($Fe^{II}CO_3$). For pH < 8, the sorption of As(V) onto these mineral phases is more favorable than that of As(III) (Dixit and Hering, 2003; Sø et al., 2008; Yokoyama et al., 2009; Yokoyama et al., 2012). The reduction of As(V) into As(III) on the sediment particles can be a key parameter for the release of As(III) in pore waters, assuming that As(V) is the dominant exchangeable As species. To validate this assumption, kinetic experiments would have been be carried out by using DGT samplers with 3MP binding gel for As(III) (Bennett et al., 2011), and ferrihydrite (Österlund et al., 2010), Metsorb (Bennett et al., 2010), ZrO_2 (Sun et al., 2014) or $ZnFe_2O_4$ (Gorny et al., 2015c) binding gels for total As (Harper et al., 1998). As release in February is well correlated to DOC (R^2 ≈ 0.8), as opposed to the other periods (R^2 < 0.2). It is possible that the process of As release is impacted by the source of dissolved organic matter (DOM) as shown by Gillispie et al. (2016) during incubation experiments. To validate this assumption, it could have been useful to characterize DOM composition by molecular spectroscopy (*i.e.*, fluvic, humic and/or protein-like substances) during each campaign. Furthermore, the increase in sulfide concentrations in pore waters seems to stabilize the increasing concentrations of thio-arsenic species. This phenomenon is clearly visible in February and July, where As speciation is composed of > 20% of thio-arsenic species.

Finally, only inorganic forms of arsenic [As(III), As(V), and thio-arsenical species] were detected in pore waters. As(III) is the dominant species, with thio-arsenic species at the bottom of the cores.

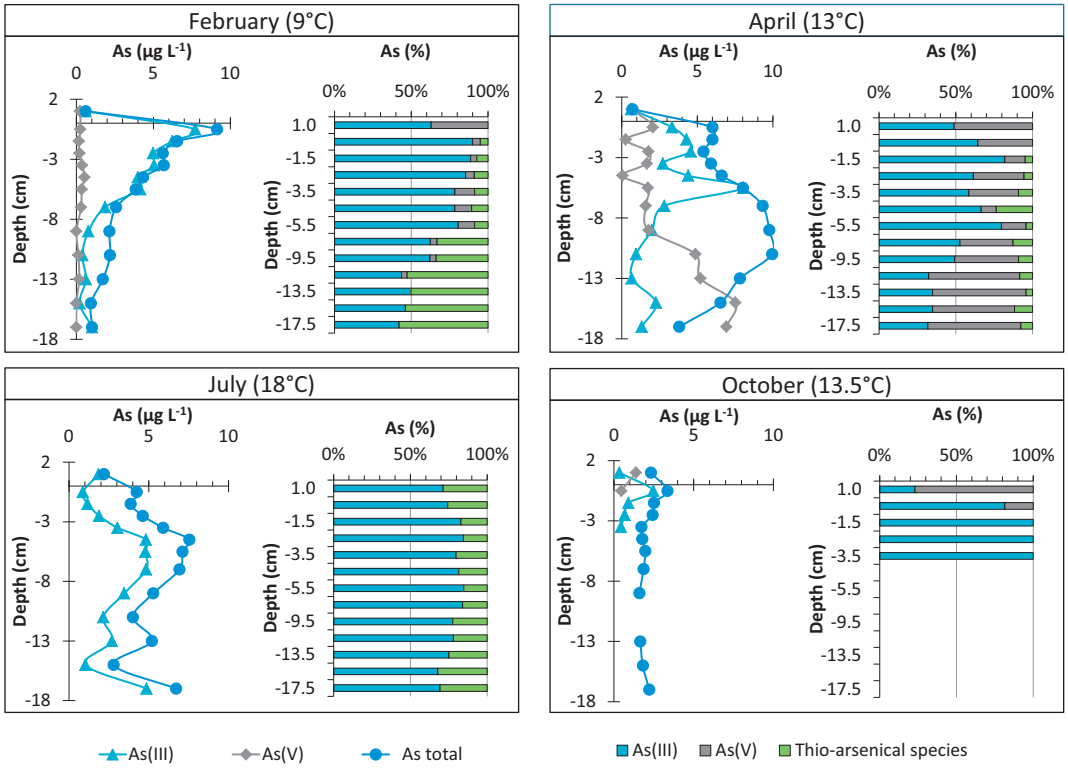

Fig. 7. Seasonal variation of total As and As species with depth in pore waters from sediment cored in the Marque River in February, April, July and October 2014. *: Calibration of the peak area of thio-arsenic species is done using the calibration slope of As inorganic species, since no standard for thio-arsenic species is commercially available.

No particular correlation can be established between total dissolved concentrations of As, Fe, and Mn, thus suggesting there is no direct redox interaction between these three elements. According to these results, As cycle may be rather linked to the sulfur cycle, and more particularly to the production of dissolved sulfides by the sulfate-reducing bacteria. No trace of methylated species was detected in pore waters (detection limit lower than 0.5 µg L^{-1}), suggesting that bacterial methylation processes are negligible in the Marque River sediments.

4. Conclusion

This study has focused on the fate of As in anoxic sediments of the Marque River. The first key point shows that the values of redox potential cannot be used as input data for thermodynamic modelling. Indeed, some major redox sensitive species are electrochemically inactive onto the surface of the Pt electrode. This observation supports that experimental redox speciation studies are required to well characterize the behaviour of As species in pore waters. Nevertheless, it is possible to use the redox potential values (coupled with pH measurement) as a qualitative proxy for the reduction of iron (hydr)-oxides in surface sediments.

In addition, temporal monitoring has permitted to follow the changes in As speciation in the sediments. Arsenic is present only under inorganic forms in pore waters, *i.e.*, As(III), As(V) and thio-arsenic species. Changes in As speciation in the dissolved phase depend mainly on S(-II) production by sulfate-reducing bacteria, which makes the amount of dissolved S(-II) an important parameter to control the fate of As in anoxic sediments. As(III) is the dominant species, with thio-arsenic species at the bottom of the cores. However, a special attention must be paid in the future to the identification of these species. The solid phase contains a substantial fraction of exchangeable As, whose presence is supported by the fact that pore waters are undersaturated with respect to arsenic pentoxide ($As^{V}_{2}O_5$), arsenolite ($As^{III}_{2}O_3$), claudelite ($As^{III}_{2}O_3$) and orpiment ($As^{III}_{2}S_3$). Several host minerals are responsible of As sorption in the sediments of the Marque River, such as amorphous iron and manganese (hydr)-oxides, calcite ($CaCO_3$) and siderite ($Fe^{II}CO_3$). Further environmental studies should focus on (i) the identification of sorption mechanisms between As species and secondary minerals formed in river sediments, with the aim to confirm that the retention of As(III) is low; and (ii) on the determination of the thio-arsenic species in the anoxic pore waters.

Acknowledgments

The authors would like to acknowledge Andra and Région Hauts-de-France for the PhD funding of Josselin Gorny. The study was also carried out in the framework of the CPER CLIMIBIO project with financial supports from the Region Hauts-de-France and the French Government.

Appendix A. Supplementary data

Supplementary data to this article can be found online at https://doi.org/10.1016/j.gexplo.2018.01.021.

References

Alexandratos, V.G., Elzinga, E.J., Reeder, R.J., 2007. Arsenate uptake by calcite: macroscopic and spectroscopic characterization of adsorption and incorporation mechanisms. Geochim. Cosmochim. Acta 71, 4172–4187.
Alvarez-Ayuso, E., Garcia-Sanchez, A., 2003. Removal of heavy metals from waste waters by natural and Na-exchanged bentonites. Clay Clay Miner. 51, 475–480.
Álvarez-Ayuso, E., García-Sánchez, A., Querol, X., 2007. Adsorption of Cr(VI) from synthetic solutions and electroplating wastewaters on amorphous aluminium oxide. J. Hazard. Mater. 142, 191–198.
Ammann, A.A., Rüttimann, T.B., Bürgi, F., 2000. Simultaneous determination of TOC and TNb in surface and wastewater by optimised high temperature catalytic combustion. Water Res. 34 (14), 3573–3579.
Appelo, C., Van der Weiden, M., Tournassat, C., Charlet, L., 2002. Surface complexation of ferrous iron and carbonate on ferrihydrite and the mobilization of arsenic. Environ. Sci. Technol. 36, 3096–3103.
Atteia, O., 1994. Major and trace elements in precipitation on western Switzerland. Atmos. Environ. 28, 3617–3624.
Ayoub, G.M., Mehawej, M., 2007. Adsorption of arsenate on untreated dolomite powder. J. Hazard. Mater. 148, 259–266.

Bennett, W.W., Teasdale, P.R., Panther, J.G., Welsh, D.T., Jolley, D.F., 2010. New diffusive gradients in a thin film technique for measuring inorganic arsenic and selenium (IV) using a titanium dioxide based adsorbent. Anal. Chem. 82, 7401–7407.
Bennett, W.W., Teasdale, P.R., Panther, J.G., Welsh, D.T., Jolley, D.F., 2011. Speciation of dissolved inorganic arsenic by diffusive gradients in thin films: selective binding of AsIII by 3-mercaptopropyl-functionalized silica gel. Anal. Chem. 83, 8293–8299.
Berner, R.A., 1980. Early Diagenesis: A Theoretical Approach. Princeton University Press.
Besra, L., Sengupta, D., Roy, S., 2000. Particle characteristics and their influence on dewatering of kaolin, calcite and quartz suspensions. Int. J. Miner. Process. 59, 89–112.
Billon, G., Ouddane, B., Boughriet, A., 2001. Chemical speciation of sulfur compounds in surface sediments from three bays (Fresnaye, Seine and Authie) in northern France, and identification of some factors controlling their generation. Talanta 53, 971–981.
Billon, G., Ouddane, B., Proix, N., Desormieres, J., Abdelnour, Y., Boughriet, A., 2005. Distribution coefficient and redox behaviour of uranium in Authie Bay (northern France). Int. J. Environ. Anal. Chem. 85, 1013–1024.
Borch, T., Kretzschmar, R., Kappler, A., Cappellen, P.V., Ginder-Vogel, M., Voegelin, A., et al., 2009. Biogeochemical redox processes and their impact on contaminant dynamics. Environ. Sci. Technol. 44, 15–23.
Bose, P., Sharma, A., 2002. Role of iron in controlling speciation and mobilization of arsenic in subsurface environment. Water Res. 36, 4916–4926.
Bostick, B.C., Fendorf, S., 2003. Arsenite sorption on troilite (FeS) and pyrite (FeS2). Geochim. Cosmochim. Acta 67, 909–921.
Boughriet, A., Proix, N., Billon, G., Recourt, P., Ouddane, B., 2007. Environmental impacts of heavy metal discharges from a smelter in Deûle-canal sediments (northern France): concentration levels and chemical fractionation. Water Air Soil Pollut. 180, 83–95.
Bout-Roumazeilles, V., Cortijo, E., Labeyrie, L., Debrabant, P., 1999. Clay mineral evidence of nepheloid layer contributions to the Heinrich layers in the northwest Atlantic. Palaeogeogr. Palaeoclimatol. Palaeoecol. 146, 211–228.
Bowell, R.J., 1994. Sorption of arsenic by iron oxides and oxyhydroxides in soils. Appl. Geochem. 9, 279–286.
Callahan, J., Dai, M., Chen, R.F., Li, X., Lu, Z., Huang, W., 2004. Distribution of dissolved organic matter in the Pearl River Estuary, China. Mar. Chem. 89 (1), 211–224.
Canfield, D., 1988. Sulfate Reduction and the Diagenesis of Iron in Anoxic Marine Sediments. Yale University.
Chaillou, G., Schäfer, J., Anschutz, P., Lavaux, G., Blanc, G., 2003. The behaviour of arsenic in muddy sediments of the Bay of Biscay (France). Geochim. Cosmochim. Acta 67, 2993–3003.
Chao, T., Zhou, L., 1983. Extraction techniques for selective dissolution of amorphous iron oxides from soils and sediments. Soil Sci. Soc. Am. J. 47, 225–232.
Charriau, A., Lesven, L., Gao, Y., Leermakers, M., Baeyens, W., Ouddane, B., et al., 2011. Trace metal behaviour in riverine sediments: role of organic matter and sulfides. Appl. Geochem. 26, 80–90.
Churchill, H., Teng, H., Hazen, R.M., 2004. Correlation of pH-dependent surface interaction forces to amino acid adsorption: implications for the origin of life. Am. Mineral. 89, 1048–1055.
Cooper, D.C., Morse, J.W., 1998. Extractability of metal sulfide minerals in acidic solutions: application to environmental studies of trace metal contamination within anoxic sediments. Environ. Sci. Technol. 32, 1076–1078.
Couture, R.-M., Gobeil, C., Tessier, A., 2010. Arsenic, iron and sulfur co-diagenesis in lake sediments. Geochim. Cosmochim. Acta 74, 1238–1255.
Deng, T., Wu, Y., Yu, X., Guo, Y., Chen, Y.-W., Belzile, N., 2014. Seasonal variations of arsenic at the sediment–water interface of Poyang Lake, China. Appl. Geochem. 47, 170–176.
Dixit, S., Hering, J.G., 2003. Comparison of arsenic(V) and arsenic(III) sorption onto iron oxide minerals: implications for arsenic mobility. Environ. Sci. Technol. 37, 4182–4189.
Drahota, P., Rohovec, J., Filippi, M., Mihaljevic, M., Rychlovský, P., Cervený, V., et al., 2009. Mineralogical and geochemical controls of arsenic speciation and mobility under different redox conditions in soil, sediment and water at the Mokrsko-West gold deposit, Czech Republic. Sci. Total Environ. 407, 3372–3384.
Fabian, D., Zhou, Z., Wehrli, B., Friedl, G., 2003. Diagenetic cycling of arsenic in the sediments of eutrophic Baldeggersee, Switzerland. Appl. Geochem. 18, 1497–1506.
Floroiu, R.M., Davis, A.P., Torrents, A., 2004. Kinetics and mechanism of As2S3(am) dissolution under N2. Environ. Sci. Technol. 38, 1031–1037.
Gagnon, C., Mucci, A., Pelletier, É., 1995. Anomalous accumulation of acid-volatile sulphides (AVS) in a coastal marine sediment, Saguenay Fjord, Canada. Geochim. Cosmochim. Acta 59, 2663–2675.
Gao, Y., Lesven, L., Gillan, D., Sabbe, K., Billon, G., De Galan, S., et al., 2009. Geochemical behavior of trace elements in sub-tidal marine sediments of the Belgian coast. Mar. Chem. 117, 88–96.
Gillispie, E.C., Andujar, E., Polizzotto, M.L., 2016. Chemical controls on abiotic and biotic release of geogenic arsenic from Pleistocene aquifer sediment to groundwater. Environ. Sci.: Processes Impacts 18, 1090–1103.
Gorny, J., Billon, G., Lesven, L., Dumoulin, D., Madé, B., Noiriel, C., 2015a. Arsenic behavior in river sediments under redox gradient: a review. Sci. Total Environ. 505, 423–434.
Gorny, J., Dumoulin, D., Lesven, L., Noiriel, C., Madé, B., Billon, G., 2015b. Development and application of a HPIC-ICP-MS method for the redox arsenic speciation in river sediment pore waters. J. Anal. At. Spectrom. 30, 1562–1570.
Gorny, J., Lesven, L., Billon, G., Dumoulin, D., Noiriel, C., Pirovano, C., et al., 2015c. Determination of total arsenic using a novel Zn-ferrite binding gel for DGT techniques: application to the redox speciation of arsenic in river sediments. Talanta 144, 890–898.
Grabowski, L.A., Houpis, J.L.J., Woods, W.I., Johnson, K.A., 2001. Seasonal bioavailability of sediment-associated heavy metals along the Mississippi river floodplain. Chemosphere 45, 643–651.
Gustafsson, J., 1991. Visual MINTEQ ver. 3.0. KTH Department of Land and Water Resources Engineering, Stockholm, Sweden. Based on de Allison JD, Brown DS, Novo-Gradac KJ, MINTEQA2 ver 2011. 4.
Haese, R., Schramm, J., Van Der Loeff, M.R., Schulz, H., 2000. A comparative study of iron and manganese diagenesis in continental slope and deep sea basin sediments off Uruguay (SW Atlantic). Int. J. Earth Sci. 88, 619–629.
Han, D.S., Song, J.K., Batchelor, B., Abdel-Wahab, A., 2013. Removal of arsenite(As(III)) and arsenate(As(V)) by synthetic pyrite (FeS2): synthesis, effect of contact time, and sorption/desorption envelopes. J. Colloid Interface Sci. 392, 311–318.
Harper, M.P., Davison, W., Zhang, H., Tych, W., 1998. Kinetics of metal exchange between solids and solutions in sediments and soils from DGT fluxes. Geochim. Cosmochim. Acta 62, 2757–2770.
Héduit, A., 1989. Potentiel d'électrode de platine en épuration biologique des eaux. Etudes ressources en eau CEMAGREF. 1.
Hongxia, Z., Yongxin, X., Zuyi, T., 2005. Sorption of uranyl ions on gibbsite: effects of contact time, pH, ionic strength, concentration and anion of electrolyte. Colloids Surf. A Physicochem. Eng. Asp. 252, 1–5.
Hussain, S.A., Demirci, Ş., Özbayoğlu, G., 1996. Zeta potential measurements on three clays from Turkey and effects of clays on coal flotation. J. Colloid Interface Sci. 184, 535–541.
Ivanovsky, A., Criquet, J., Dumoulin, D., Alary, C., Prygiel, J., Duponchel, L., et al., 2016. Water quality assessment of a small peri-urban river using low and high frequency monitoring. Environ. Sci.: Processes Impacts 18, 624–637.
Jain, C.K., Ali, I., 2000. Arsenic: occurrence, toxicity and speciation techniques. Water Res. 34, 4304–4312.
Jensen, D.L., Boddum, J.K., Tjell, J.C., Christensen, T.H., 2002. The solubility of rhodochrosite (MnCO3) and siderite (FeCO3) in anaerobic aquatic environments. Appl. Geochem. 17, 503–511.
Jones, B., Turki, A., 1997. Distribution and speciation of heavy metals in surficial sediments from the Tees Estuary, north-east England. Mar. Pollut. Bull. 34, 768–779.
Jönsson, J., Sherman, D.M., 2008. Sorption of As(III) and As(V) to siderite, green rust (fougerite) and magnetite: implications for arsenic release in anoxic groundwaters. Chem. Geol. 255, 173–181.
Jørgensen, B., 2006. Bacteria and marine biogeochemistry. In: Schulz, H., Zabel, M. (Eds.), Marine Geochemistry. Springer, Berlin Heidelberg, pp. 173–207.
Keon, N.E., Swartz, C.H., Brabander, D.J., Harvey, C., Hemond, H.F., 2001. Validation of an arsenic sequential extraction method for evaluating mobility in sediments. Environ. Sci. Technol. 35, 2778–2784.
Kostka, J.E., Luther, G.W., 1994. Partitioning and speciation of solid phase iron in salt-marsh sediments. Geochim. Cosmochim. Acta 58, 1701–1710.
Kostka, J.E., Luther, G.W., Nealson, K.H., 1995. Chemical and biological reduction of Mn (III)-pyrophosphate complexes: potential importance of dissolved Mn(III) as an environmental oxidant. Geochim. Cosmochim. Acta 59, 885–894.
Lesven, L., 2008. Devenir des éléments traces métalliques au sein du sédiment, un compartiment clé de l'environnement aquatique Ecole doctorale des SMRE Université de Lille 1.
Lesven, L., Gao, Y., Billon, G., Leermakers, M., Ouddane, B., Fischer, J.C., et al., 2008. Early diagenetic processes aspects controlling the mobility of dissolved trace metals in three riverine sediment columns. Sci. Total Environ. 407, 447–459.
Li, Y., Schoonmaker, J., 2003. Chemical Composition and Mineralogy of Marine Sediments: Na.
Louriño-Cabana, B., Lesven, L., Charriau, A., Billon, G., Ouddane, B., Boughriet, A., 2011. Potential risks of metal toxicity in contaminated sediments of Deûle river in Northern France. J. Hazard. Mater. 186, 2129–2137.
Luoma, S.N., Rainbow, P.S., Luoma, S., 2008. Metal Contamination in Aquatic Environments: Science and Lateral Management. Cambridge University Press.
Marmier, N., Delisée, A., Fromage, F., 1999. Surface complexation modeling of Yb(III), Ni (II), and Cs(I) sorption on magnetite. J. Colloid Interface Sci. 211, 54–60.
Metzger, E., 2004. Processus de transfert benthique du cadmium dans deux écosystèmes côtiers, la Baie de Sepetiba (RJ Brésil) et l'Etang de Thau (34-France). Université Paris VII Denis Diderot, France, pp. 250 (Thesis).
Meyer, D., Prien, R.D., Dellwig, O., Waniek, J.J., DE, Schulz–Bull, 2014. Electrode measurements of the oxidation reduction potential in the Gotland Deep using a moored profiling instrumentation. Estuar. Coast. Shelf Sci. 141, 26–36.
Morse, J.W., Luther III, G.W., 1999. Chemical influences on trace metal-sulfide interactions in anoxic sediments. Geochim. Cosmochim. Acta 63, 3373–3378.
Nealson, K.H., 1997. Sediment bacteria: who's there, what are they doing, and what's new? Annu. Rev. Earth Planet. Sci. 25, 403–434.
Orero Iserte, L., Roig-Navarro, A.F., Hernández, F., 2004. Simultaneous determination of arsenic and selenium species in phosphoric acid extracts of sediment samples by HPLC-ICP-MS. Anal. Chim. Acta 527, 97–104.
Österlund, H., Chlot, S., Faarinen, M., Widerlund, A., Rodushkin, I., Ingri, J., et al., 2010. Simultaneous measurements of As, Mo, Sb, V and W using a ferrihydrite diffusive gradients in thin films (DGT) device. Anal. Chim. Acta 682, 59–65.
Páez-Espino, D., Tamames, J., de Lorenzo, V., Cánovas, D., 2009. Microbial responses to environmental arsenic. BioMetals 22, 117–130.
Peiffer, S., Klemm, O., Pecher, K., Hollerung, R., 1992. Redox measurements in aqueous solutions—a theoretical approach to data interpretation, based on electrode kinetics. J. Contam. Hydrol. 10, 1–18.
Prygiel, É., 2013. Impact des remises en suspension du sédiment liées au trafic fluvial en rivières canalisées sur l'état des masses d'eau: application au bassin Artois-Picardie. Lille. 1.
Rickard, D., 2006. The solubility of FeS. Geochim. Cosmochim. Acta 70, 5779–5789.
Rochette, E.A., Bostick, B.C., Li, G., Fendorf, S., 2000. Kinetics of arsenate reduction by dissolved sulfide. Environ. Sci. Technol. 34, 4714–4720.

Romero, M.F., Armienta, A.M., Carrillo-Chavez, A., 2004. Arsenic sorption by carbonate-rich aquifer material, a control on arsenic mobility at Zimapán, México. Arch. Environ. Contam. Toxicol. 47, 1–13.
Roosa, S., 2013. Bacterial Communities in Metal Contaminated Sediments. University of Mons (pp. 220 p).
Ruban, V., López-Sánchez, J., Pardo, P., Rauret, G., Muntau, H., Quevauviller, P., 2001. Development of a harmonised phosphorus extraction procedure and certification of a sediment reference material. J. Environ. Monit. 3, 121–125.
Sadiq, M., 1995. Arsenic chemistry in soils: an overview of thermodynamic predictions and field observations. Water Air Soil Pollut. 93, 117–136.
Salameh, Y., Al-Lagtah, N., Ahmad, M.N.M., Allen, S.J., Walker, G.M., 2010. Kinetic and thermodynamic investigations on arsenic adsorption onto dolomitic sorbents. Chem. Eng. J. 160, 440–446.
Salinas-Nolasco, M.F., Méndez-Vivar, J., Lara, VcH, Bosch, P., 2004. Passivation of the calcite surface with malonate ion. J. Colloid Interface Sci. 274, 16–24.
Schulz, H.D., Zabel, M., 2006. Marine Geochemistry. vol. 2 Springer.
Singh, J., Huang, P., Hammer, U., Liaw, W., 1996. Influence of citric acid and glycine on the adsorption of mercury(II) by kaolinite under various pH conditions. Clay Clay Miner. 44, 41–48.
Sø, H.U., Postma, D., Jakobsen, R., Larsen, F., 2008. Sorption and desorption of arsenate and arsenite on calcite. Geochim. Cosmochim. Acta 72, 5871–5884.
Stefánsson, A., Arnórsson, S., Sveinbjörnsdóttir, Á.E., 2005. Redox reactions and potentials in natural waters at disequilibrium. Chem. Geol. 221, 289–311.
Sterckeman, T., Douay, F., Fourrier, H., Proix, N., 2002. Référentiel pédo-géochimique du Nord-Pas de Calais (Rapport final et annexes. Arras). .
Sterckeman, T., Douay, F., Baize, D., Fourrier, H., Proix, N., Schvartz, C., et al., 2006. Trace element distributions in soils developed in loess deposits from northern France. Eur. J. Soil Sci. 57, 392–410.
Sun, M.-Y., Dai, J., 2005. Relative influences of bioturbation and physical mixing on degradation of bloom-derived particulate organic matter: clue from microcosm experiments. Mar. Chem. 96, 201–218.
Sun, Q., Chen, J., Zhang, H., Ding, S., Li, Z., Williams, P.N., et al., 2014. Improved diffusive gradients in thin films (DGT) measurement of total dissolved inorganic arsenic in waters and soils using a hydrous zirconium oxide binding layer. Anal. Chem. 86, 3060–3067.
Teasdale, P.R., Hayward, S., Davison, W., 1999. In situ, high-resolution measurement of dissolved sulfide using diffusive gradients in thin films with computer-imaging densitometry. Anal. Chem. 71, 2186–2191.
Vershinin, A.V., Rozanov, A.G., 1983. The platinum electrode as an indicator of redox environment in marine sediments. Mar. Chem. 14, 1–15.
Wang, S., Mulligan, C.N., 2008. Speciation and surface structure of inorganic arsenic in solid phases: a review. Environ. Int. 34, 867–879.
Weatherburn, M., 1967. Phenol-hypochlorite reaction for determination of ammonia. Anal. Chem. 39, 971–974.
Wenzel, W.W., Kirchbaumer, N., Prohaska, T., Stingeder, G., Lombi, E., Adriano, D.C., 2001. Arsenic fractionation in soils using an improved sequential extraction procedure. Anal. Chim. Acta 436, 309–323.
Wilk, P.A., Shaughnessy, D.A., Wilson, R.E., Nitsche, H., 2005. Interfacial interactions between Np(V) and manganese oxide minerals manganite and hausmannite. Environ. Sci. Technol. 39, 2608–2615.
Wolthers, M., Charlet, L., van Der Weijden, C.H., van der Linde, P.R., Rickard, D., 2005. Arsenic mobility in the ambient sulfidic environment: sorption of arsenic(V) and arsenic(III) onto disordered mackinawite. Geochim. Cosmochim. Acta 69, 3483–3492.
Xu, H., Allard, B., Grimvall, A., 1991. Effects of acidification and natural organic materials on the mobility of arsenic in the environment. Water Air Soil Pollut. 57–58, 269–278.
Yokoyama, Y., Mitsunobu, S., Tanaka, K., Itai, T., Takahashi, Y., 2009. A study on the coprecipitation of arsenite and arsenate into calcite coupled with the determination of oxidation states of arsenic both in calcite and water. Chem. Lett. 38, 910–911.
Yokoyama, Y., Tanaka, K., Takahashi, Y., 2012. Differences in the immobilization of arsenite and arsenate by calcite. Geochim. Cosmochim. Acta 91, 202–219.
Yolcubal, I., Akyol, N.H., 2008. Adsorption and transport of arsenate in carbonate-rich soils: coupled effects of nonlinear and rate-limited sorption. Chemosphere 73, 1300–1307.
Zaman, M.I., Mustafa, S., Khan, S., Xing, B., 2009. Effect of phosphate complexation on Cd^{2+} sorption by manganese dioxide (β-MnO_2). J. Colloid Interface Sci. 330, 9–19.
Zhang, J., Kim, H., Townsend, T., 2014. Methodology for assessing thioarsenic formation potential in sulfidic landfill environments. Chemosphere 107, 311–318.